

# An approach to the structure determination of nucleic acid analogues hybridized to RNA. NMR studies of a duplex between 2'-OMe RNA and an oligonucleotide containing a single amide backbone modification

M.J.J. Blommers\*, U. Pieleš<sup>1</sup> and A. De Mesmaeker<sup>1</sup>

Physics and <sup>1</sup>Central Research, Ciba-Geigy AG, PO Box, CH-4002 Basel, Switzerland

Received June 21, 1994; Revised and Accepted August 26, 1994

## ABSTRACT

The backbone modification *amide-3*, in which  $-\text{CH}_2\text{-NH-CO-CH}_2-$  replaces  $-\text{C}_5'\text{H}_2\text{-O}_5'\text{-PO}_2\text{-O}_3'-$ , is studied in the duplex  $d(\text{G}_1\text{-C}_2\text{-G}_3\text{-T}_4\text{-T}_5\text{-G}_6\text{-C}_7\text{-G}_8) \cdot \text{mr}(\text{C}_9\text{-G}_{10}\text{-C}_{11}\text{-A}_{12}\text{-A}_{13}\text{-C}_{14}\text{-G}_{15}\text{-C}_{16})$  where  $\cdot$  indicates the backbone modification and *mr* indicates the 2'-OMe RNA strand. The majority of the exchangeable and non-exchangeable resonances have been assigned. The assignment procedure differs from standard methods. The methyl substituent of the 2'-OMe position of the RNA strand can be used as a tool in the interpretation. The duplex structure is a right-handed double helix. The sugar conformations of the 2'-OMe RNA strand are predominantly N-type and the 2'-OMe is positioned at the surface of the minor groove. In the complementary strand, only the sugar of residue  $\text{T}_4$  is found exclusively in N-type conformation. The incorporation of the amide modification does not effect very strongly the duplex structure. All bases are involved in Watson-Crick base pairs.

## INTRODUCTION

Investigation of conformational changes observed by NMR spectroscopy upon substitution of nucleoside analogues in oligonucleotides may guide the design of new unnatural antisense oligonucleotides (1,2). The first studies of this kind are carried out using a model DNA duplex, in which a single modification is inserted in the centre of the duplex. NMR studies of a DNA duplex where one phosphate has been replaced by a formacetal linkage (3) or a thioformacetal linkage (4) and a DNA duplex where one D-deoxyribose has been replaced by a L-deoxyribose (5) have been reported recently.

Recently, we described the replacement of the phosphodiester backbone in antisense oligonucleotides by amide linkages (6). The five possible amide dimers have been incorporated into oligonucleotides. The amide backbone modification depicted in Figure 1 has shown a significant increased affinity to a complementary RNA strand ( $\Delta T_{m/\text{modification}} = +0.4^\circ$

compared with the corresponding DNA strand; 6–8). Moreover, the amide linkages result in a protection of the neighbouring phosphodiester bonds against 3'-exonucleases (7). The increased affinity to RNA, together with the enhanced stability against nucleases, prompted us to introduce these new modifications into biologically relevant sequences. In order to gain some information about the geometrical features of the amide modifications, these were investigated by means of molecular modelling (7). In this paper we describe NMR studies of a duplex containing the *amide-3* modification (cf. Figure 1).

Previously mentioned NMR studies of nucleic acid analogues were carried out on modified oligonucleotides complexed to DNA oligonucleotides (B-type duplexes). Since the antisense oligonucleotides are intended to bind to messenger RNA molecules, a more relevant system is a duplex involving a RNA oligonucleotide. In the current investigation, we have studied the duplex formed between a 2'-OMe RNA strand and a deoxyribose oligonucleotide containing a single amide backbone modification in the centre.

The decision to use 2'-OMe substituted RNA was dictated by the greater resistance of the corresponding oligonucleotides towards nucleases and also by an easier solid-phase synthesis compared with the natural RNA. Subsequently, we found that the 2'-OMe substituent also facilitated the analysis of the NMR spectra.

## MATERIALS AND METHODS

### Oligonucleotide synthesis and purification

The oligodeoxyribonucleotides and 2'-OMe oligoribonucleotides were synthesized on an automated DNA synthesizer ABI 394B (Applied Biosystems Foster City, USA) using  $\beta$ -cyanoethyl phosphoramidites and 2'-OMe  $\beta$ -cyanoethyl phosphoramidites (Glen Research USA) and standard synthesis protocols (9). In case of the 2'-OMe building blocks the coupling time was increased to 12 min. The oligonucleotides were purified by reversed phase HPLC with 4,4'-dimethoxytrityl 'ON' using a RPC18 column (4.6 × 250 mm, ODS Hypersil Shandon Runcorn,

\*To whom correspondence should be addressed

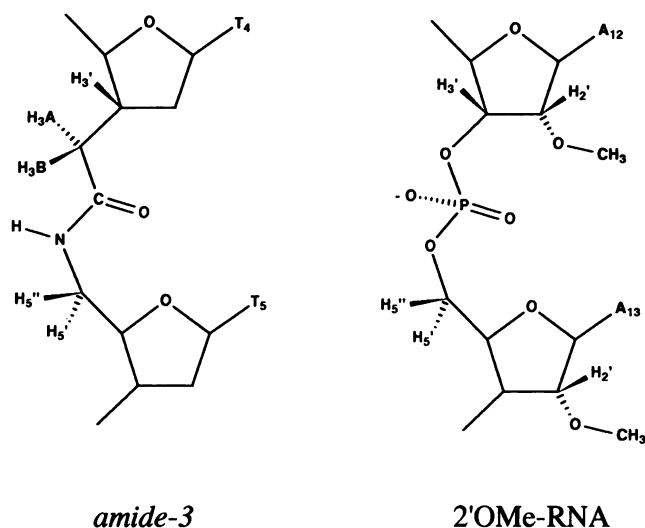


**Figure 1.** Schematic drawings of the backbone modification *amide-3* and the 2'-OMe ribose analogue. Only the important atoms are indicated together with the used nomenclature. The O-PO<sub>2</sub>-O moiety (right) has been replaced by NH-CO-CH<sub>2</sub> in the amide backbone modification (left).

UK) eluted with a linear gradient from 15 to 45% B in 45 min (eluent A: 50 mM triethylammonium acetate pH 7; eluent B: 50 mM triethylammonium acetate pH 7 in 70% acetonitrile). After removal of the remaining DMT group with 80% acetic acid and extraction with diethyl ether, the oligonucleotides were lyophilized twice from 50% aqueous ethanol to remove residual acetic acid. The purity of the oligonucleotides was then checked by capillary electrophoresis using polyacrylamide gel filled capillaries (10). The identity was confirmed by MALDI TOF mass spectrometry (11).

### NMR experiments

Most experiments were carried out using a sample of the duplex d(G-C-G-T·T-G-C-G)\*mr(C-G-C-A-A-C-G-C) with a final concentration of 3.4 mM in 10 mM phosphate buffer, pH 7.0, 100 mM NaCl, 0.05 mM EDTA. The experimental conditions were chosen in order to avoid specific mono- or multivalent ion effects (EDTA: no Mg<sup>2+</sup>). The 'D<sub>2</sub>O sample' was obtained after lyophilization and redissolving the sample mentioned above in D<sub>2</sub>O. The sample contained an approximate 10% excess of the d-strand, which improves the quality of the spectra drastically. The percentage of the excess was determined by UV absorbance measurements. The interpretation of the NMR spectra was not negatively influenced by the presence of the signals of excess monomer.

Most homonuclear 2D experiments of the sample were recorded using a Varian Unity 500 spectrometer operating at a frequency of 500 MHz. All 2D experiments were recorded at 25°C. NOESY experiments (12) were recorded with a mixing time of 75, 200 and 400 ms, respectively. Clean TOCSY experiments (13,14) were recorded with a mixing time varying from 15 to 75 ms. Non-selective T<sub>1</sub>-relaxation measurements were carried out using the inversion-recovery method. The phase-sensitive 2D spectra were recorded with 400 experiments and 2048 complex data points using quadrature detection in both dimensions (15). A double-quantum filtered (2QF) COSY experiment (16) was recorded with 512 experiments and 4096

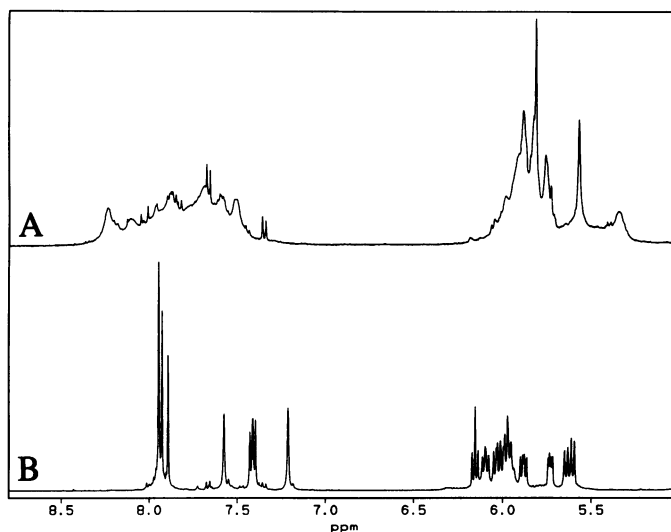


**Figure 2.** One-dimensional NMR spectra (aromatic and H1' sugar <sup>1</sup>H resonances) of the oligonucleotides mr(C-G-C-A-A-C-G-C) (A) and d(G-C-G-T·T-G-C-G) (B) before mixing. The spectra are recorded after dissolving the sample in D<sub>2</sub>O, pH = 7.0. The samples are annealed for 10 min at 50°C, 1 h prior to the measurements.

complex data points. A NOESY experiment with the duplex dissolved in water (H<sub>2</sub>O:D<sub>2</sub>O = 95:5) was recorded on a Bruker AMX600 spectrometer with a non-selective observation pulse as described before (17) using a mixing time of 200 ms. <sup>31</sup>P spectra were recorded on a Bruker AM400 spectrometer, interfaced with an Aspect3000 computer.

Data were transferred to a Silicon Graphics workstation and processed with the software package FELIX 2.05 purchased from BIOSYM. The 2D data sets were treated by shifted sine bell or Gaussian filters and zero filled up to 1024 data points in the t<sub>1</sub> dimension. Distance-geometry calculations were carried out using DGII (18). Energy minimization was performed with Discover (BIOSYM) using the AMBER force field (19).

## RESULTS AND DISCUSSION

### Characterization and conditions probing

A section of the 1D NMR spectra of the oligonucleotides d(G-C-G-T·T-G-C-G) and mr(C-G-C-A-A-C-G-C) is shown in Figure 2. The resonances of the 2'-OMe RNA strand are unexpectedly broad (cf. Figure 2A), and the number of signals exceeds the number of protons present in the monomer octamer. This observation results from the (unexpected) formation of aggregates. One-dimensional spectra have been measured in a 10 times diluted, i.e., 0.3 mM 2'-OMe RNA sample and at elevated temperatures up to 50°C. Under all of these conditions a very broad and complex spectrum is observed. The spectrum of d(G-C-G-T·T-G-C-G) (cf. Figure 2B) has the normal characteristics expected for a single-stranded octamer.

One-dimensional spectra of a 1:1 mixture of both oligonucleotides are presented in Figure 3. The resonance at approximately 6.7 p.p.m. is not present in either of the spectra of the single strand oligonucleotides (cf. Figure 2), a normally empty region between the aromatic and the H1' resonances. This is typical for a duplex structure. This resonance is not shifted significantly by a small raise in the temperature but it broadens

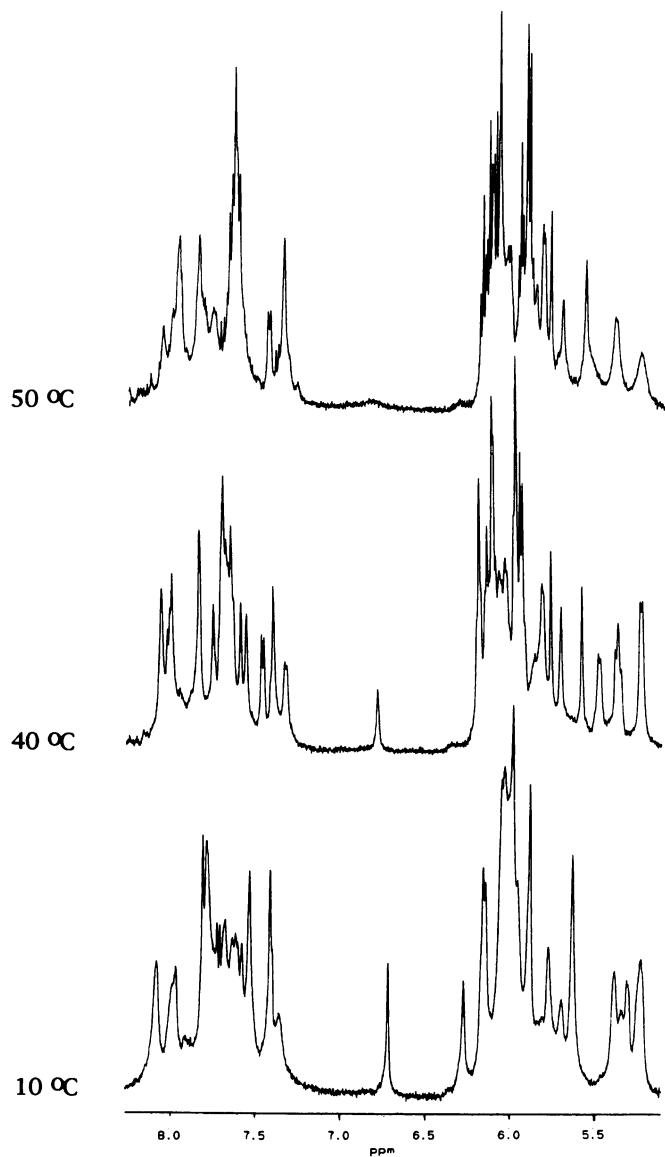


Figure 3. One dimensional NMR spectra of the duplex d(G-C-G-T·T-G-C-G)\*mr(C-G-C-A-A-C-G-C) in D<sub>2</sub>O at 10, 40 and 50°C.

at about 50°C. This indicates that at the latter temperature the duplex structure is in intermediate exchange with the aggregate formed by self-association of the RNA strand.

In addition, the line width of the H5 resonances (5–5.5 p.p.m.) increases between 40 and 50°C. The relative intensity of the isolated resonance around 6.7 p.p.m. measured in the spectrum recorded at 40°C is smaller than that of the other resonances. This implies that a minor fraction of the 2'-OMe RNA is present as aggregate at this temperature. All temperature effects are reversible. The quality of the spectra was improved by adding a 10% excess of the DNA strand. All further experiments of this sample are carried out at 25°C. Under these conditions, the isolated resonance around 6.7 p.p.m. has the same integrated intensity as the other resonances.

After optimizing the conditions for measuring the duplex d(G-C-G-T·T-G-C-G)\*mr(C-G-C-A-A-C-G-C) a preliminary

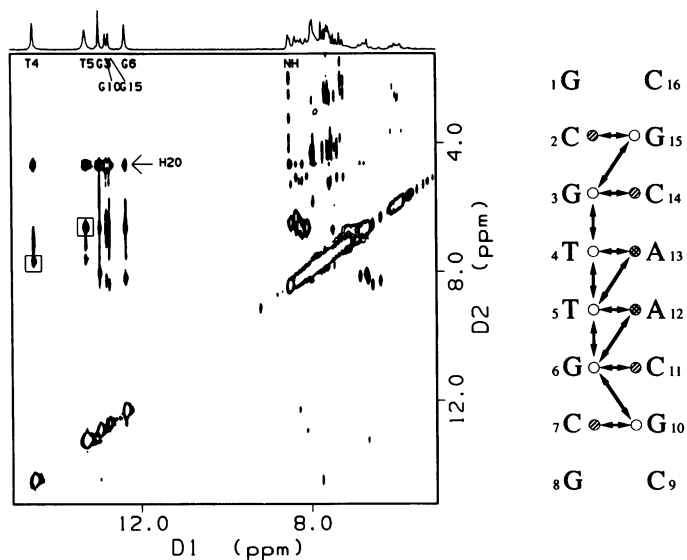


Figure 4. NOESY spectrum of the duplex d(G-C-G-T·T-G-C-G)\*mr(C-G-C-A-A-C-G-C) in 95% H<sub>2</sub>O/5% D<sub>2</sub>O recorded with a mixing time of 200 ms. The assignment of the NH–H<sub>2</sub> cross peaks are highlighted by boxes. The connectivities involving the exchangeable protons in 1D and 2D NOE experiments are shown in the right panel. Open, dashed and dotted circles denote NH, NH<sub>2</sub> and H<sub>2</sub> protons, respectively.

characterization of this duplex is useful. Because of the unknown effects of the 2'-OMe substituent and the incorporated amide linkage it is difficult to decide whether the assignment can be done by following methods used for A- and B-type helices (20–22).

The <sup>1</sup>H spectrum of the duplex recorded in 95% H<sub>2</sub>O/5% D<sub>2</sub>O is shown in Figure 4 on top of a NOESY spectrum recorded with a mixing time of 200 ms. Both spectra were obtained without presaturation of the water signal and allow the observation of the exchangeable proton resonances. All imino protons resonate between 12 and 15 p.p.m., which indicates their involvement in base pairing. The signals of particular interest are the imino proton resonances of residues T<sub>4</sub> and T<sub>5</sub>, which might be affected by the amide backbone. These imino proton resonances can be assigned easily by the appearance of strong cross peaks involving signals at 6.73 and 7.8 p.p.m., presumably aromatic proton resonances. The interpretation of the D<sub>2</sub>O spectra, supplemented with T<sub>1</sub> relaxation data, will prove that these resonances are H<sub>2</sub> resonances (*vide infra*). The complete interpretation of the NOESY spectrum supplemented by 1D NOE experiments obtained after irradiation of each imino proton signal, result in the assignment of imino and amino proton resonances listed in Table 1 as well as the NOE connectivity table presented in Figure 4, right panel. The NH resonance of the amide backbone modification is not visible in the spectrum, because it resonates in very close proximity to one of the amino protons. However, strong NOEs are observed between this amide proton resonance and the methylene backbone proton resonances, which can be assigned independently in the D<sub>2</sub>O spectra (*vide infra*).

In the TOCSY spectrum of the duplex recorded at room temperature (not shown) six cross peaks are observed, which represent the six H<sub>5</sub>–H<sub>6</sub> connectivities of the four cytidines in the 2'-OMe ribose strand and two in the deoxyribose strand. The intensities are almost equal and no other cross peaks are observed.

**Table 1.** Resonance assignment of the duplex d(G<sub>1</sub>-C<sub>2</sub>-G<sub>3</sub>-T<sub>4</sub>·T<sub>5</sub>-G<sub>6</sub>-C<sub>7</sub>-G<sub>8</sub>)\*mr(C<sub>9</sub>-G<sub>10</sub>-C<sub>11</sub>-A<sub>12</sub>-A<sub>13</sub>-C<sub>14</sub>-G<sub>15</sub>-C<sub>16</sub>) at 25°C in ppm relative to DSS

	NH	NH <sub>2</sub>	H6,8	H2,5	H1' Me	H2'	H2''	H3'	H4' OMe	H5',5''
G <sub>1</sub>			8.02		6.05	2.81	2.81	4.81	4.25	
C <sub>2</sub>		8.54, 6.65	7.65	5.43	6.10	2.68	2.64	4.84	4.35	
G <sub>3</sub>	13.05		7.53		6.04	2.75	2.80	4.65	4.34	4.22
T <sub>4</sub>	14.61		7.71	1.31	5.78	2.07	2.21	2.56	4.06	4.12
T <sub>5</sub>	13.38		7.38	1.63	5.95	2.37	2.76	4.66	4.34	3.38,3.98
G <sub>6</sub>	12.43		7.74		5.99	2.52	2.71	4.92	4.40	4.16,4.24
C <sub>7</sub>		8.44, 6.46	7.31	5.22	6.02	2.20	2.54	4.80	(4.26)	(4.16)
G <sub>8</sub>			7.67		6.17	2.41	2.41	4.60	(4.36)	(4.14,4.17)
C <sub>9</sub>			8.00	5.94	5.71	4.25	3.67			
G <sub>10</sub>	12.88		7.79		5.97	4.39	3.81			
C <sub>11</sub>		8.35, 6.73	7.68	5.35	5.69	4.44	3.68	(4.51)	(4.25)	
A <sub>12</sub>			8.06	6.73	6.11	4.43	3.81	4.51	4.24	(4.48)
A <sub>13</sub>			8.01	7.80	6.21	4.21	3.77	4.48	4.18	
C <sub>14</sub>		8.19, 6.78	7.46	5.22	5.58	4.07	3.63	4.44	4.37	
G <sub>15</sub>	12.83		7.57		5.94	3.99	3.76			
C <sub>16</sub>			7.62	5.32	5.90	3.73	3.51			
H3A	2.14									
H3B	2.67									

This indicates that the major species in solution at this temperature is the duplex.

Several cross peaks are observed corresponding with the H1'–H2' and H1'–H2'' spin pairs in the deoxy-oligomer. Most cross peaks are present at this short mixing time, which indicates that the sugars have either an S-type conformation or are found in an equilibrium between N-type and S-type.

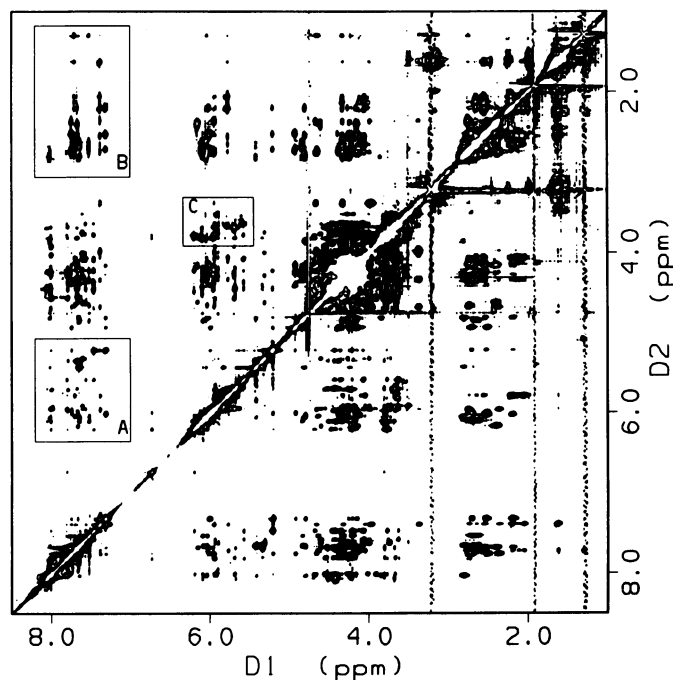
Cross peaks between H1' and H2' of the 2'-OMe riboses ought to be found at about 4–6 p.p.m. No cross peaks of this kind are observed, which indicates that the sugars have strong preference for the N-type conformation.

Figure 5 shows the NOESY spectrum of the duplex dissolved in D<sub>2</sub>O. The comparison of region A of the NOESY spectrum displayed in Figure 3 and the same spectral region in the TOCSY spectrum (not shown) reveals that the strong cross peaks observed in region A correspond to the cytidine H5–H6 connectivities (distance 2.5 Å). All cross peaks between resonances of H1' and aromatic protons which may be observed in this region can merely be observed in the same region of the NOESY spectrum recorded with a mixing time of 75 ms (not shown), whereas cross peaks between the H2' and H2'' resonances and aromatic protons (Figure 3, Box B) give rise to strong nuclear Overhauser effects. These observations reflect an anti orientation of the bases in agreement with a Watson–Crick base pair formation.

Although the generalization of the findings mentioned above for all nucleotides in the duplex is questionable, it is assumed that the structure of the duplex share characteristics of A- or B-type duplexes. This is used for the resonance assignment.

The assignment of NMR resonances of oligonucleotides usually starts in the region of the cross peaks between H1' resonances and H6 or H8 resonances (20–22). The observed cross peaks are very weak at short mixing times, i.e. near the detection limit, but after prolonged mixing time, spin diffusion is mediated by the H2' and H2'' spins and cross peaks can be detected in this region (cf. Figure 5, region A). This region shows a high peak density and is therefore not very suitable to start a sequential assignment.

Region B and C (Figure 5) are selected to start the sequential assignment. Region B is attractive to start the assignment of the deoxyribose strand, because no signals of the 2'-OMe RNA



**Figure 5.** NOESY spectrum of the duplex d(G-C-G-T·T-G-C-G)\*mr(C-G-C-A-A-C-G-C) in D<sub>2</sub>O recorded with a mixing time of 400 ms. Regions B and C can be used for the resonance assignment, since they correspond to one strand only: DNA (B) or 2'-OMe RNA (C). Region C is magnified in Figure 6. Region A is enlarged in Figure 9.

strand are present in this region. Region C is very suitable because, apart from some putative cross peaks with backbone proton resonances, it only contains cross peaks between 2'-OMe and H1' resonances corresponding to the protons in the 2'-OMe RNA strand.

#### Assignment of the resonances of the 2'-OMe ribose nucleosides

In region C of Figure 5 pairs of cross peaks are observed which easily can be connected via a sequential assignment (cf. Figure

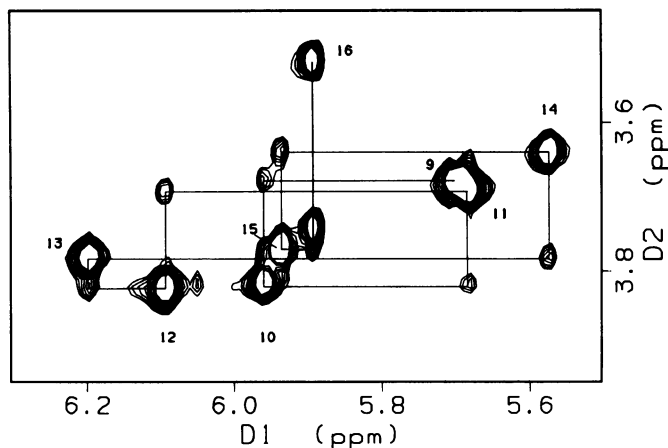


**Figure 6.** Part of the NOESY spectrum recorded with a mixing time of 400 ms in which cross peaks are found between 2'-OMe resonances and H1' resonances. This region permits a sequential assignment of these resonances in the 2'-OMe RNA strand mr(C<sub>9</sub>-G<sub>10</sub>-C<sub>11</sub>-A<sub>12</sub>-A<sub>13</sub>-C<sub>14</sub>-G<sub>15</sub>-C<sub>16</sub>). The corresponding structure and connectivities are drawn in Figure 8.

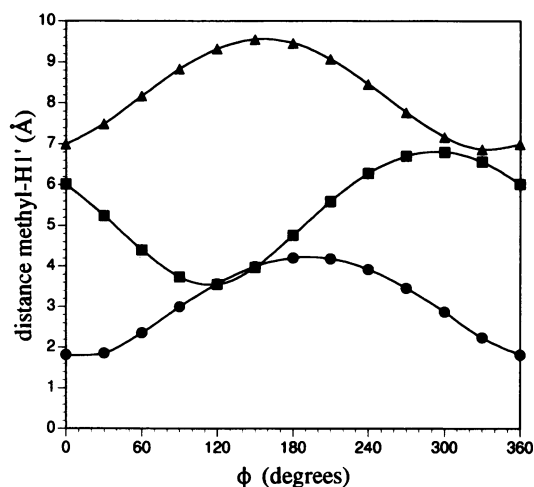


**Figure 7.** Distances calculated between the average position of the 2'-OMe protons and the H1' protons in an A-type helix as a function of the orientation of the methyl group. The distances are plotted as a function of the torsion angle  $\phi$  (C1'-C2'-O2'-CH<sub>3</sub>). OMe(i)-H1'(i-1): triangles, OMe(i)-H1'(i): dots, OMe(i)-H1'(i+1): boxes.

6). Strong cross peaks are detected which can be connected via very weak cross peaks, indicating intra residue H1'-OMe contacts (strong cross peaks) and the inter residue H1'-OMe contacts. Because of the unknown conformation of the nucleotides, in particular the orientation of the 2'-OMe group relative to the sugar, the weak cross peak may either originate from OMe(i)-H1'(i-1) or from OMe(i)-H1'(i+1) connectivities. Since the structure of the 2'-OMe strand is close to that of an A-type helix (*vide infra*) a model of an A-type helix is generated. In this model the distance between the H1' proton and the average position of the three methyl protons is calculated as a function of the rotation around the torsion angle  $\phi$  (C1'-C2'-O2'-CH<sub>3</sub>). This calculation is performed for the three possible combinations, i.e. OCH<sub>3</sub>(i)-H1'(i-1), OCH<sub>3</sub>(i)-H1'(i) and OCH<sub>3</sub>(i)-H1'(i+1).

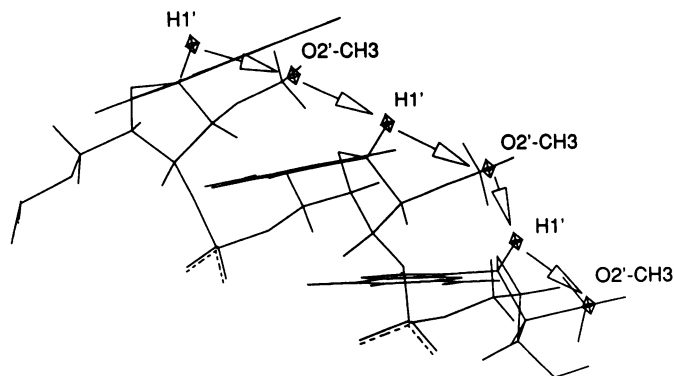


**Figure 8.** The inter-residual and intra-residual H1' atoms and 2'-OMe moieties can be connected via a sequential walk in the A-type helix when the methyl is directed into the minor groove. This structure corresponds to the sequential cross peak analysis of Figure 6.

The results are displayed in Figure 7. These model calculations indicate that the combination (i,i-1) results for all values of  $\phi$  in a distance larger than 7 Å and is therefore not further considered. (i,i) reflects the combination which corresponds to a large cross peak, since the distance can be smaller than 3 Å. Then, the weak cross peaks should correspond to the (i,i+1) connectivities. The observation that for each 2'-OMe two cross peaks (weak and strong) are observed in this region is in agreement with a gauche(+) conformation around  $\phi$ , i.e. the methyl occupies a position at the surface of the minor groove. This conformation of the 2'-OMe sugar analogue finds corroboration by an independent study by X-ray diffraction (Egli, personal communication).

Following the analysis described above it is now possible to assign all cross peaks in Figure 6. For example, the cross peak designated A<sub>12</sub> is the A<sub>12</sub>OMe-A<sub>12</sub>H1' cross peak, whereas the tiny cross peak at the same frequency (3.79 p.p.m.) is the A<sub>12</sub>OMe-A<sub>13</sub>H1' cross peak. Subsequently, the sequential connectivity walk can be performed as indicated in Figure 6 and illustrated in the structure shown in Figure 8.

Based on the H1' assignments described above, these results can be extended to the part of the NOESY spectrum where cross peaks between H1' resonances and aromatic proton resonances are found. Such an analysis can now readily be performed as is shown in Figure 9A. The sequential assignment is consistent with the H<sub>6,8</sub>(i)-H<sub>5</sub>(i+1) cross peaks observed in the same region, which confirms the assignment of the four H<sub>5</sub>-H<sub>6</sub> cross peaks. Finally, the assignment is extended to the H<sub>2</sub>' resonances.

#### Assignment of the resonances of the deoxyribose nucleotides

The resonance assignment of the deoxyribose nucleosides can be performed by a sequential assignment involving the cross peaks of region B (Figure 5). In such a sequential assignment cross peaks are connected corresponding to the short intra-strand H<sub>6,8</sub>-H<sub>2</sub>' and H<sub>6,8</sub>-H<sub>2</sub>'' distances and those corresponding to the short intra-residue H<sub>6,8</sub>(i+1)-H<sub>2</sub>'(i) and H<sub>6,8</sub>(i+1)-H<sub>2</sub>''(i) distances, which are expected for a A- or B-type structure. In addition to that, the results of the TOCSY and 2QF-COSY experiments are used to identify cross peaks involving H<sub>5</sub> and H<sub>6</sub> of cytidines and cross peaks between the methyl proton resonances and thymidine H<sub>6</sub> resonances.

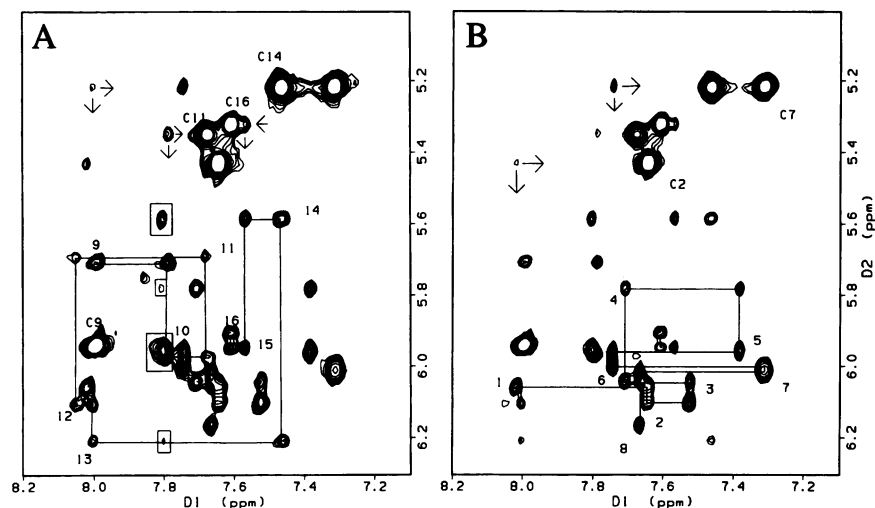


**Figure 9.** Part of the NOESY spectrum of the duplex  $d(G_1-C_2-G_3-T_4 \cdot T_5-G_6-C_7-G_8) \cdot mr(C_9-G_{10}-C_{11}-A_{12}-A_{13}-C_{14}-G_{15}-C_{16})$  recorded with a mixing time of 400 ms corresponding to box A in Figure 5. After the assignment of the H2'/H2'' and aromatic proton resonances of the DNA strand and after the assignment of the H1' and 2'-OMe resonances of the RNA strand, cross peaks between the H1' and H6,8 resonances can be identified, unambiguously. The sequential analysis is indicated. The numbers correspond to the intra-residual H1'–H6,8 cross peaks. Cn indicates H5–H6 cross peaks which are also present in the TOCSY experiment. The arrows indicate the H5(i+1)–H8(i) cross peaks. The boxed cross peaks in the left plot are assigned to H2–H1' cross peaks.

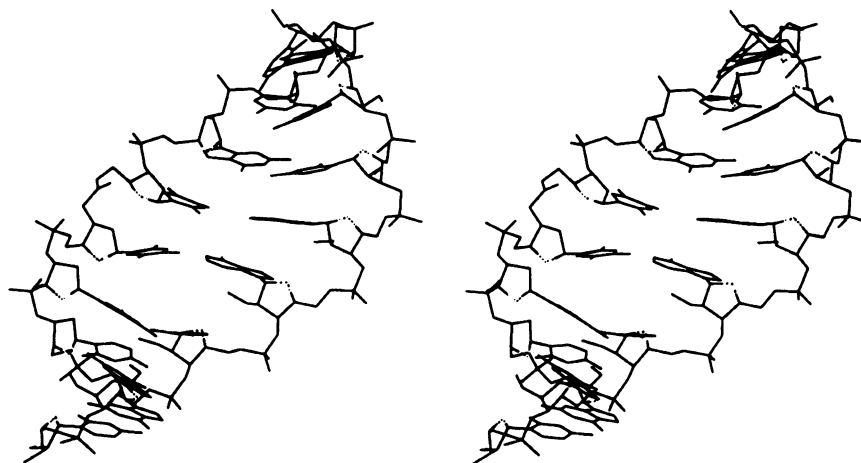


**Figure 10.** Stereo view of a crude model of the structure of the duplex  $d(G-C-G-T \cdot T-G-C-G) \cdot mr(C-G-C-A-A-C-G-C)$  obtained by distance-geometry and energy minimization. Sugar O4' atom bonds are indicated by dotted lines. The protons are not shown. The left half of the structure displays the deoxyribose strand with the amide backbone modification inserted between the two central thymidines. The 2'-OMe RNA strand is shown in the right half. The 2'-OMe groups are orientated towards the minor groove.

The assignment of the H2' and H2'' resonances is extended with the assignment of the H1' and H3' resonances. Here the H1'–H2', H2'' connectivities in NOESY are located in the 2QF-COSY and TOCSY spectra. The assignments of the aromatic resonances and H1' resonances are shown in Figure 9B and show consistency. The H2' and H2'' resonances finally are assigned stereo specifically, considering the differences in the distance between these protons and the H1' proton of the same residue. Except for the cross peaks involving T<sub>4</sub>H1', the NOEs have similar intensities (H1'–H2': 0.37 and H1'–H2'': 0.47; 200 ms mixing time) and the NOESY recorded at 75 ms mixing time is necessary to obtain an unambiguous stereo specific assignment.

Finally, the assignment finds corroboration by the data obtained from the 2QF-COSY spectrum. No cross peak is found for H1'–H2' of this residue, which is connected by a very small  $J_{1'2'}$ . The minimal value for  $J_{1'2'}$  is about 1–2 Hz. The cross peak attribution for H1'–H2'' is straightforward, since the minimal value calculated for  $J_{1'2'}$  is 4–5 Hz. The sugar of residue T<sub>4</sub> which is connected to the amide backbone is found to occur almost exclusively in an N-type conformation. The results of the assignment are collected in Table 1. In some favourable case the assignment is extended to those of the backbone proton resonances as well. In summary, all contacts between H6,8(i) and H1'(i–1) are observed. All contacts between

**Table 2.**  $T_1$  relaxation rates in seconds of the duplex d(G<sub>1</sub>-C<sub>2</sub>-G<sub>3</sub>-T<sub>4</sub>·T<sub>5</sub>-G<sub>6</sub>-C<sub>7</sub>-G<sub>8</sub>)\*mr(C<sub>9</sub>-G<sub>10</sub>-C<sub>11</sub>-A<sub>12</sub>-A<sub>13</sub>-C<sub>14</sub>-G<sub>15</sub>-C<sub>16</sub>)

	H6, H8	H2, H5	H1'	OCH3
G <sub>1</sub>	1.4	—	—	—
C <sub>2</sub>	(1.2)	1.9	1.9	—
G <sub>3</sub>	1.4	—	—	—
T <sub>4</sub>	1.8	—	1.9	—
T <sub>5</sub>	1.7	—	—	—
G <sub>6</sub>	1.3	—	—	—
C <sub>7</sub>	1.3	2.0	—	—
G <sub>8</sub>	(1.4)	—	1.7	—
C <sub>9</sub>	2.3	—	2.5	2.2
G <sub>10</sub>	2.3	—	—	2.2
C <sub>11</sub>	(1.4)	1.7	2.5	2.2
A <sub>12</sub>	1.4	4.0	—	2.0
A <sub>13</sub>	2.0	3.6	2.5	2.3
C <sub>14</sub>	2.0	2.0	2.6	2.3
G <sub>15</sub>	2.3	—	2.3	—
C <sub>16</sub>	2.3	2.8	2.5	1.7

H8(i) and H5(i+1) are found as well as the contact between T<sub>4</sub>H8 and T<sub>5</sub>CH<sub>3</sub>. The expected NOE between G<sub>3</sub>H8 and T<sub>4</sub>CH<sub>3</sub> is not detected at 200 ms mixing time, but a cross peak appears in the NOESY spectrum, recorded with 400 ms. Finally, all contacts are observed between H6,8(i) and H2'/H2''(i-1), with the exception of the following: no discrimination can be made between the important connectivities G<sub>3</sub>H2'-T<sub>4</sub>H6 and G<sub>3</sub>H2''-T<sub>4</sub>H6, because of a degeneracy of these H2' and H2'' resonances. Because T<sub>4</sub>H3' is part of the spin system of the backbone modification it has been shifted upfield. Connectivities are found with the H2' and H2'' resonances as well as with the H4' resonance in TOCSY and 2QF-COSY experiments.

In addition to the H6,8-H1' cross peaks, four cross peaks in the region displayed in Figure 9 cannot be assigned to a H6,8-H1' contact. The same is apparent for the isolated resonance around 6.7 p.p.m. The two aromatic proton resonances which are not discussed yet are assigned to the two adenosine H2 protons. In an A- or B-type helix these protons have a position in the centre of the helix, close to the helix axis, whereas the H6, H8 and sugar resonances are positioned relatively far away from the helix axis. In a B-type helix, the first H1' atom which is in the vicinity of a H2 proton is more than 4.5 Å apart from H2. Short H2-H1' distances are diagnostic for an A-type helix. It is well known that the  $T_1$ -relaxation rates of H2 resonances are significantly longer than those of the other aromatic proton resonances. This is confirmed by  $T_1$ -relaxation time measurements (*vide infra*) and by the assignment of the imino protons outlined above.

Although the sequential assignment can be performed, a careful analysis of the intensities of the intra residual cross peak intensities, e.g. those of G<sub>3</sub>, T<sub>4</sub> and T<sub>5</sub>, indicates that the middle part of the duplex deviates from the regular A- or B-type helix.

The <sup>31</sup>P spectrum of the duplex (not shown) is similar to that expected for an unperturbed DNA:RNA duplex. All resonances are found in a narrow spectral region of 1 p.p.m. This indicates that none of the backbone torsion angles  $\alpha$  and  $\zeta$  have switched from a gauche(-) conformation to a trans conformation.

### $T_1$ relaxation times

The relaxation rates obtained from non-selective  $T_1$ -experiments of the duplex are given in Table 2. The relaxation rates indicate a significant difference between the  $T_1$  times of the H6/H8

resonances and H1' resonances of the two different strands: the average value for the d(G-C-G-T·T-G-C-G) strand is 1.4 and 1.8 for the aromatic and H1' signals, respectively, whereas the average value for the mr(C-G-C-A-A-C-G-C) strand are 2.0 and 2.5 s for the same type of protons. The  $T_1$  values measured in both strands are

$$T_{1av}(\text{d-strand})/T_{1av}(\text{mr-strand}) = 0.78$$

This observation is probably connected with differences in internal motions of the two strands. Conclusions cannot be made yet, since also cross relaxation effects are determining the  $T_1$  values. Similar effects have been observed by RNA:DNA hybrids before (23).

### Structure calculations

The observations described above prompted us for the generation of a crude structural model based on the data discussed in the previous sections. Such a crude model is generated by means of distance-geometry calculations. Standard Watson-Crick base pairs are assumed, N-type sugar conformations are defined for residue T<sub>4</sub> as well as for all 2'-OMe riboses. All other sugars are restrained to an S-type conformation. The NOE connectivities described in this paper are converted in upper bound distances of 5 Å. Twenty structures are generated and the best structure has been subjected to energy minimization using the AMBER force field. This structure is presented in Figure 10.

This model encompasses pretty well the observations described in the previous sections: it demonstrates that although the amide backbone may have local effects on the structure, the overall structure is relatively unperturbed. Apart from the region in the vicinity of the amide backbone, the structural features of the duplex are quite similar to those found for DNA-RNA hybrids (24). It should be mentioned, that details of the perturbation caused by the insertion of the amide backbone can only be obtained after a relaxation matrix analysis of the NOEs and an elucidation of the torsion angles in the molecule. This work is currently in progress.

### CONCLUSIONS

Model duplex molecules are proposed to study the structure of nucleic acid analogues complexed to RNA. The structure of the 2'-OMe RNA:DNA hybrid studied in the current investigation is a right-handed helical duplex. All bases are involved in Watson-Crick base pairs. The sugars of the 2'-OMe RNA strand are found in an N-type conformation. Only the sugar of residue T<sub>4</sub> in the deoxyribose strand is N-type. The conformation of the latter mentioned sugar is induced by the presence of the amide backbone at the 3'-end of this sugar.

The structure of the 2'-OMe RNA strand shows structural similarities to the A-type helix. Therefore it is obvious that the 2'-OMe analogue of RNA is a good model for RNA itself. Furthermore, no interactions are found between the 2'-OMe group and the complementary strand. The use of 2'-OMe RNA instead of RNA has many advantages. It is stable against enzymes, the synthesis is easier and it has been demonstrated here that the resonance assignment is facilitated and less ambiguous due to the presence of 2'-OMe H1' connectivities.

### ACKNOWLEDGEMENT

Mrs C.Langer is thanked for technical assistance.

## REFERENCES

1. Uhlmann, E. and Peyman, A. (1990) *Chem. Rev.* **90**, 543–584.
2. Thuong, N.T. and Hélène, C. (1993) *Angew. Chem. Int. Ed. Engl.* **32**, 666–690.
3. Gao, X., Brown, F.K., Jeffs, P., Bischofberger, N., Lin, K-Y., Pipe, A.J. and Noble, S.A. (1992) *Biochemistry* **31**, 6228–6236.
4. Gao, X. and Jeffs, P.W. (1994) *J. Biomol. NMR* **4**, 17–34.
5. Blommers, M.J.J., Capobianco, M.L., Colonna, F.P., Tondelli, L. and Garbesi, A. (1993) *J. Mol. Graphics* **11**, 265.
6. De Mesmaeker, A., Lebreton, J., Waldner, A., Cook, P.D. (1992) Backbone modified oligonucleotide analogues, International patent WO 92/20, 823
7. De Mesmaeker, A., Waldner, A., Lebreton, J., Hoffmann, P., Fritsch, V., Wolf, R.M., Freier, S.M. (1994) *Angew. Chem. Int. Ed. Engl.* **33**, 226–229.
8. De Mesmaeker, A., Lebreton, J., Waldner, A., Fritsch, V., Wolf, R.M., Freier, S.M. (1993) *Synlett.* 733–736.
9. Atkinson, J. and Smith, M. (1984) In Gait, M.J. (ed.) *Oligonucleotide Synthesis: A practical approach*. IRL Press, Oxford, pp. 35–81.
10. Engelhardt, H., Beck, W., Kohr, J. and Schmitt, T. (1993) *Angew. Chem. Int. Ed. Engl.* **105**, 659–680.
11. Pieles, U., Zürcher, W., Schär, M. and Moser, H.E. (1993) *Nucleic Acids Res.* **21**, 3191–3196.
12. Jeener, J., Meier, B.H., Bachmann, P. and Ernst, R.R. (1979) *J. Chem. Phys.* **71**, 4546–4593.
13. Braunschweiler, L. and Ernst, R.R. (1983) *J. Magn. Res.* **53**, 521–558.
14. Griesinger, C., Otting, G., Wüthrich, K. and Ernst, R.R. (1988) *J. Am. Chem. Soc.* **110**, 7870–7872.
15. States, D.J., Haberkorn, R.A. and Ruben, D.J. (1982) *J. Magn. Res.* **48**, 286–292.
16. Piantini, U., Sørensen, O.W. and Ernst, R.R. (1982) *J. Am. Chem. Soc.* **104**, 6800–6801.
17. Haasnoot, C.A.G. and Hilbers, C.W. (1983) *Biopolymers* **22**, 1259–1266.
18. Havel, T.F. (1991) *Prog. Biophys. Mol. Biol.* **56**, 43–78.
19. Weiner, S.J., Kollman, P.A., Ngygen, D.T. and Case, D.A. (1986) *J. Comp. Chem.* **7**, 230–235.
20. Scheek, R.M., Russo, N., Boelens, R., Kaptein, R. and van Boom, J.H. (1983) *J. Am. Chem. Soc.* **105**, 2914–2916.
21. Haasnoot, C.A.G., Westerink, H.P., van der Marel, G.A. and van Boom, J.H. (1983) *J. Biomol. Struct. Dyns.* **1**, 131–149.
22. Hare, D.R., Wemmer, D.E., Chou, S-H., Drobny, G. and Reid, B.R. (1983) *J. Mol. Biol.* **171**, 319–336.
23. Wang, A.C., Kim, S.G., Flynn, P.F., Chou, S-H., Orban, J. and Reid, B.R. (1992) *Biochemistry* **31**, 3940–3946.
24. Hall, K.B. (1983) *Curr. Opinion Struct. Biol.* **3**, 336–339.